Phase-field Modeling of Nucleation in Solid-State Phase Transformations

Tae Wook Heo[1,*] and Long-Qing Chen[2,]**

[1]*Condensed Matter and Materials Division, Lawrence Livermore National Laboratory, Livermore, CA 94550, USA*

[2]*Department of Materials Science and Engineering, The Pennsylvania State University, University Park, PA 16802, USA*

Abstract

Nucleation is a critically important process as the rate of nucleation determines the number density of new phase particles and thus microstructures of a material during phase transformations. Predicting and controlling nucleation rates in solids is one of grand challenges in materials science due to the fact that the spatial scale involved in nucleation is at the atomic/nanoscale, the rate of nucleation process is extremely temperature sensitive, and the morphology of a critical nucleus can be highly non-spherical and complex. In this article, we briefly review the recent advances in modeling and predicting nucleation during solid phase transformations based on the diffuse-interface or non-classical description of critical nucleus profiles. The focus is on predicting the critical nucleus morphology and nucleation free energy barrier under the influence of anisotropic interfacial energy and elastic interactions. Incorporation of nucleation events in phase-field modeling of solid-to-solid phase transformations and microstructure evolution is also discussed.

[*]*e-mail*: heo1@llnl.gov

[**]*e-mail*: lqc3@psu.edu

Release number: LLNL-JRNL-650216

1. Introduction

Nucleation is a fundamental process that takes place when a material becomes metastable with respect to its phase transformation to one or more thermodynamically more stable states (Fig. 1(a)). Transformation of a metastable state to a stable one is a thermally activated process, and thus nucleation of a new phase in a metastable parent matrix requires overcoming an energy barrier. The rate of nucleation, I, is determined by two contributions, the thermodynamics, *i.e.*, the critical nucleation free energy barrier, ΔG^*, that controls the number density of critical nuclei, N^*, and the kinetics that controls the rate of growth, R, of a critical nucleus to become a stable one (Fig. 1(b)). According to the classical nucleation theory,

$$I = R \cdot N^* = R \cdot \left[N_0 \cdot \exp(-\frac{\Delta G^*}{k_B T}) \right] = I_0 \cdot \exp(-\frac{\Delta G^*}{k_B T}), \quad (1)$$

where N_0 is the number of atoms per unit volume, k_B is the Boltzmann constant, and T is the temperature. Nucleation rate is extremely temperature-sensitive with no nucleation at the transformation temperature (infinite ΔG^*) and at zero Kelvin where R is zero and a maximum in-between (Fig. 1(c)). Excellent reviews on the advances in the theoretical research of nucleation already exist [1-5]. This article will be focused on the thermodynamics of nucleation in solids, *i.e.* the nucleation barrier and the morphology of critical nuclei, as well as on how nucleation can be introduced within the context of phase-field simulations [6-11] of solid state phase transformations and microstructure evolution.

Cahn and Hilliard [12] are the first to apply the diffuse-interface model [13] to determine the critical nucleus, *i.e.*, the critical composition profile which corresponds to the minimum free energy increase or saddle point. They showed that nucleation properties become close to those predicted by the classical theory when supersaturation of a solution, *i.e.*, driving force for nucleation, is low. However, the interface between a nucleus and a parent phase becomes increasingly diffuse, and the composition of the nucleus interior becomes lower than the equilibrium composition of a new phase with increasing supersaturation. Poduri and Chen [14] extended the non-classical theory of Cahn and Hilliard [12] to describe the phase transformations involving both compositional and structural changes associated with ordering. Granasy and co-workers [8, 15-17] extensively modeled the nucleation process during solidification employing the diffuse-interface approach. Roy *et al.* [18] examined the effect of spatially nonlocal interactions on the critical nucleus profile and nucleation rate employing the phase-field

approach. Chu *et al.* [19] developed a model to study the non-classical nucleation behavior during structural transformations by introducing driving force dependencies into the interfacial energy, misfit strain energy, and nucleus chemical free energy change.

One of the challenges in phase-field method of phase transformations and microstructure evolution is to simulate the nucleation processes since the density and spatial distribution of nuclei are critical to determining the phase transformation kinetics and resultant microstructures that dictate the properties of materials. There exist two approaches to introduce nuclei within a metastable system: the Langevin noise method [20, 21] and the explicit nucleation method [22-24].

In this article, we briefly review the recent advances in theoretical and computational approach based on the diffuse-interface description to predict the critical nucleus morphology in solid-state phase transformations that involve both interfacial energy anisotropy and long-range elastic interactions as well as in simulation of nucleation in phase-field simulations of phase transformations.

2. Critical nucleus morphology and nucleation energy

The classical nucleation theory is based on the assumption that the thermodynamic properties of a nucleus are uniform and the same as the equilibrium bulk counterparts within the nucleus and the interface between the nucleus and the parent phase is sharp [25, 26]. With the assumption, the total free energy change upon the variation of the size of a nucleating particle (or *embryo*) during solid-to-solid phase transformations can be easily determined by the sum of the bulk free energy reduction, the interfacial energy increase, and the coherency strain energy increase as the following:

$$\Delta E = V \cdot (\Delta f_v + \Delta f_{coh}) + A \cdot \gamma, \tag{2}$$

where Δf_v (<0) is the bulk free energy difference between a nucleating particle and the parent phase per unit volume, Δf_{coh} (>0) is the coherency strain energy per unit volume arising from the lattice mismatch between the particle and the parent phase, and the γ is the interfacial energy per unit area between the nucleating particle and the parent phase. In this theory, the morphology of the nucleating particle is assumed *a priori*. Since V is proportional to r^3 where r is the size dimension of the nucleating particle and A is proportional to r^2, the free energy increases as the

particle grows when r is small and decreases when r is large beyond a critical value, the critical size (r^*). The energy change at the critical size is the critical nucleation energy.

In contrast to the classical theory, the non-classical theory is based on the diffuse-interface description of the interfaces (or gradient thermodynamics) [13]. The total energy change arising from a fluctuation in a phase-field variable is expressed as:

$$\Delta F = \int_{\Omega} [\Delta f(\eta) + \frac{\kappa}{2}(\vec{\nabla}\eta)^2] d^3\vec{r} + E_{coh}, \tag{3}$$

where η is the phase-field variable that can be either conserved (*e.g.*, composition) or non-conserved (*e.g.*, long-range order parameter) depending on the types of phase transformations, Δf is the variation of the local free energy upon fluctuations of the phase-field (= $f(\eta) - f(\eta_0) - (\eta - \eta_0)(\partial f / \partial \eta)_{\eta=\eta_0}$ when η is the conserved field variable, and $f(\eta) - f(\eta_0)$ when η is the non-conserved field variable), κ is the gradient energy coefficient related to the interfacial energy, and E_{coh} is the coherency strain energy arising from the lattice parameter variation upon the perturbation of phase-field variables from the homogeneous initial state.

Finding the critical nucleus morphology and the nucleation energy is to locate the saddle point on the minimum energy path (MEP) of the free energy functional landscape from the metastable state (local minimum) to the stable or equilibrium state (global minimum) [27]. The goal is to find the critical profiles of the phase-field variables that lead to the minimum free energy increase among all possible fluctuations leading to nucleation. It is a computationally expensive process since it requires the exploration of the configuration space of significantly high dimensions. However, recent advances in theory, mathematical algorithm, and computational power make it possible to explore such a high dimensional configuration space. Examples include the minimax method [28, 29], the constrained string method [30-33], the free-end nudged elastic band method [34-36], and the constrained shrinking dimer dynamics method [37-39]. It should be mentioned that the underlying principles are identical regardless of the types of methods.

Zhang, Chen, and Du [40, 41] predicted the morphology of critical nuclei and critical nucleation energy during solid to solid phase transformations employing a cubic crystal as an example taking into consideration both the anisotropic interfacial energy and the anisotropic long-range elastic interactions in both two-dimensional (2D) and three-dimensional (3D) systems by applying the minimax algorithm [28, 29] based on the mountain pass theorem without *a priori*

assumption. Mathematical and numerical details are also available in [42]. Surprisingly, it was revealed that the formation of critical nuclei with nonconvex shapes or with lower crystalline symmetries such as plates and needles than both new and parent phases are possible as shown in Fig. 2. It should be emphasized that their finding is the outcome of investigation on the unexplored regime that cannot be reached by the classical nucleation theory.

Shen, Li, and Wang [43] employed the free-end nudged elastic band method [36] to search for the critical nucleus during a cubic to tetragonal transformation. The nudged elastic band method [34, 35] is also a popular method to compute the MEPs. In contrast to the original nudged elastic band method, the free-end nudged elastic band method can take a partially transformed state rather than a product phase at equilibrium as one of end configurations, other being the initial metastable homogeneous phase, for better accuracy as well as computational efficiency. Using the Langevin fluctuations, they produced the partially transformed state as shown in Fig. 3(a) and investigated both 2D (Fig. 3(b)) and 3D (Figs. 3(c) and (d)) critical nuclei. They found that a critical nucleus consists of a single variant which has an ellipsoidal shape when the elastic contribution is low as shown in Fig. 3(c). The broad face normal is aligned with <100> crystallographic directions due to the elastic energy contribution. On the other hand, twin-related two-variant nucleus appears when the elastic contribution is high as shown in Fig. 3(d).

Zhang, Chen, and Du [33] applied the constrained string method [32] to predicting both critical nucleus and equilibrium morphologies simultaneously within the same physical model and mathematical formulation with a conservation constraint when the phase-field is a conserved variable, *e.g.*, solute composition. The constrained string method is a novel mathematical framework which is the synthesis of the original string method [30, 31] and the method of Lagrange multipliers. The constraint is enforced by the energy penalty term during the calculus of MEPs. A main difference between the nudged elastic band method and the string method is a particular term which prevents defined nodes from collapsing onto the local minima. The string method employs a particular parameterization, while the nudged elastic band method employs an artificial spring force [44]. They observed that the maximum composition in a critical nucleus can be higher or lower than that of the equilibrium state depending on the initial composition. Using the method, they investigated the elastic strain energy contribution to the nucleation energy barrier and to the shapes of the critical nucleus as well as to the equilibrium precipitate for a cubic to cubic transformation as shown in Fig. 4. The same mathematical algorithm is also

applied to exploring the critical nucleus during phase transformations involving a cubic to tetragonal crystal symmetry change for both conserved and non-conserved field variables [44]. In the case of the conserved field variable, they found that the critical nucleus and equilibrium shape depend on the stress-free transformation strain as well as on the contribution of elastic energy with respect to the chemical driving force. In the case of the non-conserved field variable, they observed that the characteristic of the critical nucleus varies from single-variant to two-variant twin structures depending on the elastic energy contribution while the equilibrium shapes are similar regardless of the elastic contribution as shown in Fig. 5.

In addition to the explained algorithms above, Zhang and Du [38, 39] developed and applied the constrained shrinking dimer dynamics method to searching for the critical nucleus profiles.

3. Nucleation in phase-field simulations

Governing equations in phase-field simulations are deterministic with the evolution of the phase-field variables towards the direction that decreases the free energy of an entire system. However, a nucleation event is stochastic and may lead to a free energy increase. Currently, two types of approaches have been employed to treat nucleation within a phase-field framework, one being the Langevin noise method [20, 21] and the other the explicit nucleation method [22-24]. The Langevin noise method incorporates the Langevin random fluctuations into the phase-field equations. The stochastic Cahn-Hilliard [45] (Eq.(4)) and Allen-Cahn [46] (Eq.(5)) equations become:

$$\frac{\partial c}{\partial t} = \vec{\nabla} \cdot M\vec{\nabla}\left(\frac{\delta F}{\delta c}\right) + \zeta(\vec{r},t), \tag{4}$$

$$\frac{\partial \eta}{\partial t} = -L\left(\frac{\delta F}{\delta \eta}\right) + \xi(\vec{r},t), \tag{5}$$

where $\zeta(\vec{r},t)$ and $\xi(\vec{r},t)$ are the random noise terms which satisfy the fluctuation-dissipation theorem [21]. The method reproduces the nucleation process well when the metastability of the initial state is small. In other words, the random noise can generate the nuclei with reasonable spatial distribution and the time scale when the metastable parent phase is close to the instability temperature or composition with respect to its transformation. There are many examples of phase-field simulations that employ the Langevin noise method. We exemplify some of representative cases in Fig. 6 [47, 48]. It is, however, difficult to generate nuclei using the

Langevin force when a system is highly metastable unless unrealistically large amplitude of noise is introduced. Since the number of nucleated particles depends on the amplitude and spatial correlation of the noise, the unrealistic large amplitude of noise may lead to overestimated or underestimated nucleation density in a system.

The explicit nucleation method is based on the classical nucleation theory [25, 26] and the Poisson seeding [22-24]. The critical nucleus size and the nucleation energy are determined by either the classical nucleation approach or the non-classical approach in section 2. The determined nuclei are explicitly incorporated into a system by assuming that the time to nucleate a new phase particle is much shorter than the computational time interval (Δt) [24]. The algorithm of the method involves the following steps [22-24, 49]: (*i*) Randomly choose a location for a nucleation site, (*ii*) Calculate a nucleation probability P $(=1-\exp(-I\cdot\Delta t))$ with the given nucleation rate I $(=I_0\exp(-\Delta G^*/k_BT))$ where I_0 is the prefactor, ΔG^* is the critical nucleation energy, k_B is the Boltzmann constant, and T is the temperature, (*iii*) Generate a uniform random number (R) between 0 and 1, (*iv*) Add a nucleus to the chosen location if P is greater than R.

Fig. 7(a) [22] shows an example of phase-field simulations with this algorithm. Shen, Simmons, and Wang [50, 51] derived the analytic form of elastic strain energy that can be directly applied to the explicit nucleation algorithm and applied them to a cubic to tetragonal structural transformation as shown in Fig. 7(b) [51]. In phase-field simulations presented in Fig. 7, the classical nuclei based on the sharp-interface description and the assumption that thermodynamic properties within a nucleus are uniform are incorporated.

Incorporating classical nuclei has two main drawbacks. First, artificial reduction of solute composition around an incorporated nucleus is required to conserve the overall composition in the case of phase transformations involving composition changes. Second, additional relaxation from the highly non-equilibrium sharp-interface to the diffuse-interface between a critical nucleus and a parent phase is required due to the diffuse-interface nature of the gradient thermodynamics within the context of the phase-field method. In order to circumvent the drawbacks, there have been efforts to incorporate non-classical nuclei in phase-field simulations. Heo *et al.* [49] discussed the explicit nucleation method for incorporating diffuse-interface critical nuclei for structural transformations predicted by the minimax algorithm [28, 29]. The order parameter profiles and nucleation energy of critical nuclei were computed, and they were

introduced to a metastable system employing the explicit nucleation algorithm in phase-field simulations. They analyzed the growth kinetics of a single non-classical nucleus as well as the overall kinetics of an entire nucleation-and-growth process. Fig. 8(a) shows the nucleation-and-growth process simulated by this method. Using the same method, the phase transformation involving compositional changes was also modeled as shown in Fig. 8(b) [52].

Recently, Li *et al.* [53] applied the non-classical nucleation method to a realistic system. They generated non-classical nuclei of a Cr precipitate in a FeCr alloy for different overall compositions and temperatures employing the constrained shrinking dimer dynamic method [38, 39] and the realistic thermodynamic database of the alloy system as shown in Figs. 9(a) and (b). They analyzed the growth kinetics of a non-classical nucleus (Fig. 9(c)) and compared it with the classical nucleus counterpart. They found several non-classical features of the growth kinetics and differences in kinetic behaviors between classical and non-classical nuclei. In addition, they confirmed that the classical nucleus requires the interface relaxation from the sharp-interface profile to the non-classical profile before its growth.

4. Conclusions

We briefly reviewed recent advances in the phase-field method for modeling nucleation in solid-state phase transformations. It includes the applications of sophisticated mathematical algorithms to locating the saddle point on the free energy functional landscape corresponding to the critical microstructural configuration of the nucleus in the presence of anisotropic interfacial energy and long-range elastic interactions. The advanced modeling techniques permit the observations of various non-classical features of nucleation. Examples include finding the critical nuclei with nonconvex shapes or with lower crystalline symmetries than both new and parent phases. In addition, it was found that the transition of critical nucleus features from single-variant to twin-related two-variant occurs with the increasing elastic interactions during the phase transformations from a high-symmetry phase to a low-symmetry phase. It was also revealed that, depending on the initial composition, the maximum composition in a critical nucleus can be either higher or lower than the equilibrium composition of a new phase when compositional evolution involves. The existing two types of methods for the dynamic nucleation in phase-field simulations were also discussed. The recent development of theoretical models and mathematical algorithms based on the diffuse-interface description has extended our understanding of the

critical nucleus in solid-to-solid phase transformations and has allowed us to find new features that could not be possible by the classical nucleation theory.

Acknowledgement

The work of T.W. Heo was performed under the auspices of the U.S. Department of Energy by Lawrence Livermore National Laboratory under Contract DE-AC52-07NA27344. This work was funded by the Laboratory Directed Research and Development Program at LLNL under project tracking code 12-ERD-053. L.Q. Chen acknowledges the financial support by NSF under CMMI-1235092 and DOE Basic Sciences under the CMCSN Program. We acknowledge the figure permissions by the American Physical Society, the Elsevier, the Springer, the Global Science Press, the Taylor & Francis, the IOP Publishing, and Dr. L. Zhang.

Figure captions

Figure 1. Schematic diagrams and illustration of (a) an energy landscape during a nucleation process, (b) conversion of a critical nucleus to a stable particle through atom attachment, and (c) nucleation rate as a function of temperature where T_0 is the transformation temperature.

Figure 2. Critical nuclei profiles in (a) 2D systems [40] (Reprinted figure with permission from [40]. Copyright 2007 by the American Physical Society.) and (b) 3D systems [41] predicted by the minimax algorithm (Reprinted with permission from [41]. Copyright 2008 by the Elsevier.).

Figure 3. (a) A partially transformed state at an earlier stage of a cubic to tetragonal transformation in a 2D system produced by the Langevin dynamics, (b) a critical nucleus configuration in a 2D system, (c) a 3D critical nucleus with the low elastic energy contribution, and (d) a 3D critical nucleus with the high elastic energy contribution predicted by the free-end nudged elastic band method [43]. Reprinted figure with permission from [43]. Copyright 2008 by the Springer.

Figure 4. Minimum energy paths with a conservation constraint showing critical nuclei and equilibrium states for different elastic energy contributions predicted by the constrained string

method [33]. Reprinted figure with permission from [33]. Copyright 2010 by the Global Science Press.

Figure 5. Application of the constrained string method to a cubic to tetragonal transformation with non-conserved phase-field variables: (a) critical nucleus and (b) equilibrium state profiles with the low elastic contribution, (c) critical nucleus and (d) equilibrium state profiles with the high elastic contribution [44]. Reprinted figure with permission from [44]. Copyright 2010 by the Elsevier.

Figure 6. Examples of nucleation driven by the Langevin noise in phase-field simulations: (a) nucleation during a *fcc* to $L1_2$ ordering process [47] (Reprinted figure with permission from [47]. Copyright 2002 by the Elsevier.) and (b) precipitate nucleation during a generic diffusional process in a polycrystalline binary solid solution [48] (Reprinted figure with permission from [48]. Copyright 2013 by the Taylor & Francis).

Figure 7. Examples of phase-field simulations of nucleation and growth with the explicit nucleation method and classical nuclei: (a) a generic nucleation and growth process [22] (Reprinted figure with permission from [22]. Copyright 2000 by the Elsevier.) and (b) a cubic to tetragonal transformation [51] (Reprinted figure with permission from [51]. Copyright 2007 by the Elsevier.).

Figure 8. Examples of phase-field simulations of nucleation and growth with the explicit nucleation method and non-classical nuclei: (a) a generic structural transformation [49] (Reprinted figure with permission from [49]. Copyright 2010 by the Elsevier.) and (b) a generic phase transformation involving composition changes [52] (Reprinted figure with permission from [52].).

Figure 9. Critical nucleus profiles computed by the constrained shrinking dimer dynamic method for (a) different overall compositions of Cr and (b) different temperatures, and (c) the growth of the nucleus at 500 K when Cr overall composition is 0.16 [53]. Reprinted figure with permission from [53]. Copyright 2014 by the IOP Publishing.

References

[1] D. W. Oxtoby, *J. Phys.-Condens. Mat.* 4, 7627 (1992).
[2] D. W. Oxtoby, *Accounts Chem. Res.* 31, 91 (1998).
[3] J. D. Gunton, *J. Stat. Phys.* 95, 903 (1999).
[4] L. Granasy and P. F. James, *J. Non-Cryst. Solids* 253, 210 (1999).
[5] D. T. Wu, L. Granasy, and F. Spaepen, *MRS Bull.* 29, 945 (2004).
[6] L. Q. Chen, *Ann. Rev. Mater. Res.* 32, 113 (2002).
[7] W. J. Boettinger, J. A. Warren, C. Beckermann, and A. Karma, *Ann. Rev. Mater. Res.* 32, 163 (2002).
[8] L. Granasy, T. Pusztai, T. Borzsonyi, G. Toth, G. Tegze, J. A. Warren, and J. F. Douglas, *J. Mater. Res.* 21, 309 (2006).
[9] H. Emmerich, *Adv. Phys.* 57, 1 (2008).
[10] N. Moelans, B. Blanpain, and P. Wollants, *CALPHAD* 32, 268 (2008).
[11] I. Steinbach, *Model. Simul. Mater. Sc.* 17 (2009).
[12] J. W. Cahn and J. E. Hilliard, *J. Chem. Phys.* 31, 688 (1959).
[13] J. W. Cahn and J. E. Hilliard, *J. Chem. Phys.* 28, 258 (1958).
[14] R. Poduri and L. Q. Chen, *Acta Mater.* 44, 4253 (1996).
[15] L. Granasy, T. Borzsonyi, and T. Pusztai, *Phys. Rev. Lett.* 88 (2002).
[16] L. Granasy, T. Pusztai, D. Saylor, and J. A. Warren, *Phys. Rev. Lett.* 98 (2007).
[17] T. Pusztai, G. Tegze, G. I. Toth, L. Kornyei, G. Bansel, Z. Y. Fan, and L. Granasy, *J. Phys.-Condens. Mat.* 20 (2008).
[18] A. Roy, J. M. Rickman, J. D. Gunton, and K. R. Elder, *Phys. Rev. E* 57, 2610 (1998).
[19] Y. A. Chu, B. Moran, A. C. E. Reid, and G. B. Olson, *Metall. Mater. Trans. A* 31, 1321 (2000).
[20] R. Kubo, *Rep. Prog. Phys.* 29, 255 (1966).
[21] E. M. Lifshitz and L. P. Pitaevskii, *Statistical physics, Part I, Landau and Lifshitz Course of Theoretical Physics* (Pergamon Press, Oxford, 1980).
[22] J. P. Simmons, C. Shen, and Y. Wang, *Scripta Mater.* 43, 935 (2000).
[23] J. P. Simmons, C. Shen, and Y. Wang, *Nucleation and Growth Processes in Materials. Symposium (Materials Research Society Symposium Proceedings Vol.580)*, 417 (2000).
[24] J. P. Simmons, Y. H. Wen, C. Shen, and Y. Z. Wang, *Mat. Sci. Eng. A-Struct.* 365, 136 (2004).
[25] D. A. Porter and K. E. Easterling, *Phase Transformations in Metals and Alloys* (Chapman & Hall, London, 1992).
[26] H. I. Aaronson and J. K. Lee, *Lectures on the theory of phase transformations* (TMS, New York, 1975).
[27] E. Wigner, *T. Faraday Soc.* 34, 0029 (1938).
[28] P. Rabinowitz, *Minimax Methods in Critical Point Theory with Applications to Differential Equations* (American Mathematical Society, Providence, RI, 1986).
[29] J. J. More and T. S. Munson, *Math. Program.* 100, 151 (2004).
[30] E. Weinan, W. Q. Ren, and E. Vanden-Eijnden, *Phy. Rev. B* 66 (2002).
[31] W. N. E, W. Q. Ren, and E. Vanden-Eijnden, *J. Chem. Phys.* 126 (2007).
[32] Q. Du and L. Zhang, *Commun. Math. Sci.* 7, 1039 (2009).
[33] L. Zhang, L.-Q. Chen, and Q. Du, *Commun. Comput. Phys.* 7, 674 (2010).
[34] G. Henkelman and H. Jonsson, *J. Chem. Phys.* 113, 9978 (2000).
[35] G. Henkelman, B. P. Uberuaga, and H. Jonsson, *J. Chem. Phys.* 113, 9901 (2000).
[36] T. Zhu, J. Li, A. Samanta, H. G. Kim, and S. Suresh, *P. Natl. Acad. Sci. USA* 104, 3031 (2007).
[37] G. Henkelman and H. Jonsson, *J. Chem. Phys.* 111, 7010 (1999).
[38] J. Zhang and Q. Du, *SIAM J. Numer. Anal.* 50, 1899 (2012).
[39] J. Zhang and Q. Du, *J. Comput. Phys.* 231, 4745 (2012).
[40] L. Zhang, L.-Q. Chen, and Q. Du, *Phys. Rev. Lett.* 98 (2007).
[41] L. Zhang, L.-Q. Chen, and Q. Du, *Acta Mater.* 56, 3568 (2008).
[42] L. Zhang, L.-Q. Chen, and Q. Du, *J. Sci. Comput.* 37, 89 (2008).

[43] C. Shen, J. Li, and Y. Z. Wang, *Metall. Mater. Trans. A* 39A, 976 (2008).
[44] L. Zhang, L.-Q. Chen, and Q. Du, *J. Comput. Phys.* 229, 6574 (2010).
[45] J. W. Cahn, *Acta Metall.* 9, 795 (1961).
[46] S. M. Allen and J. W. Cahn, *Acta Metall.* 27, 1085 (1979).
[47] V. Vaithyanathan and L. Q. Chen, *Acta Mater.* 50, 4061 (2002).
[48] T. W. Heo, S. Bhattacharyya, and L. Q. Chen, *Philos. Mag.* 93, 1468 (2013).
[49] T. W. Heo, L. Zhang, Q. Du, and L.-Q. Chen, *Scripta Mater.* 63, 8 (2010).
[50] C. Shen, J. P. Simmons, and Y. Wang, *Acta Mater.* 54, 5617 (2006).
[51] C. Shen, J. P. Simmons, and Y. Wang, *Acta Mater.* 55, 1457 (2007).
[52] L. Zhang, *Ph.D. Thesis*, The Pennsylvania State University, 2009.
[53] Y. Li, S. Hu, L. Zhang, and X. Sun, *Model. Simul. Mater. Sc.* 22, 025002 (2014).

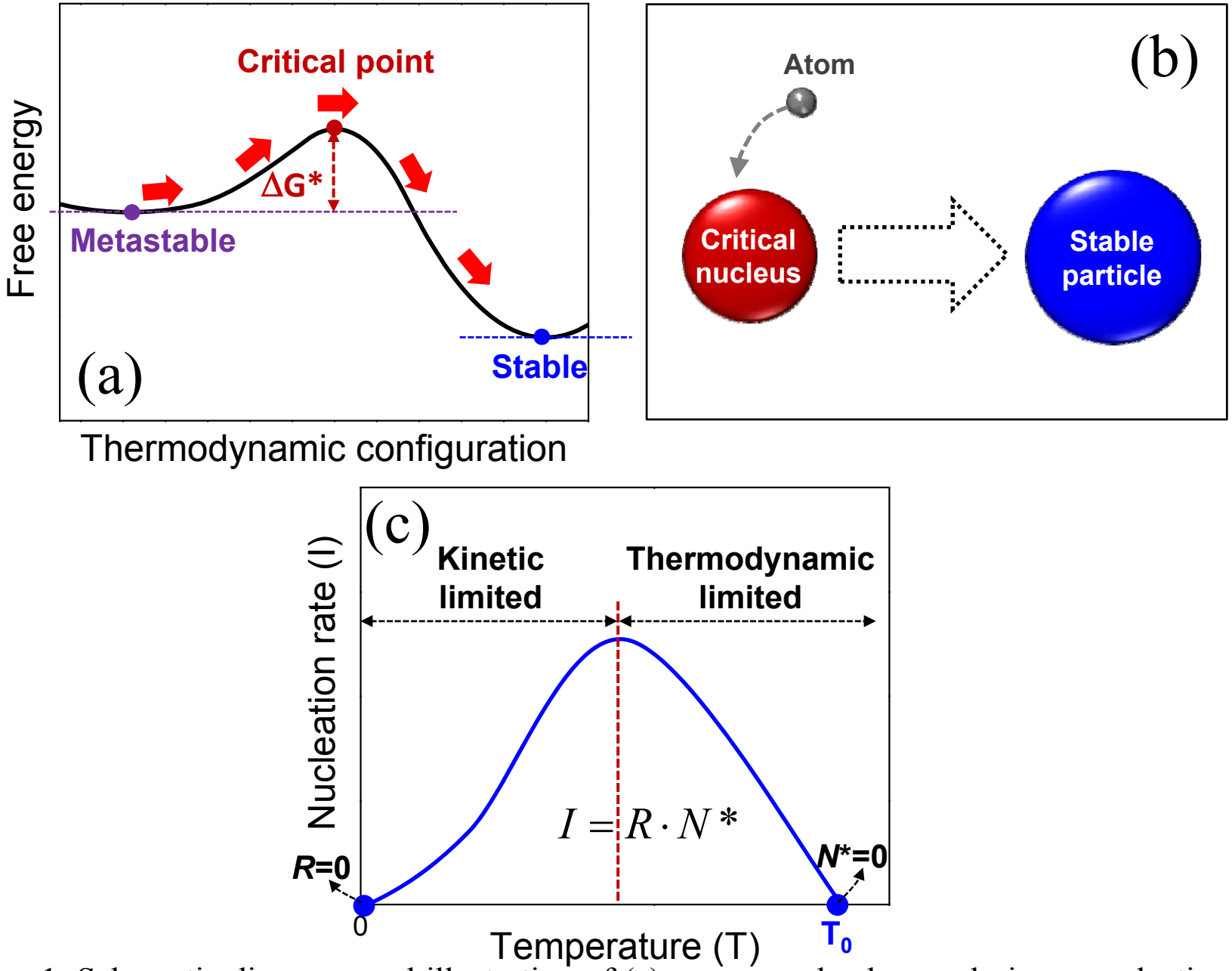

Figure 1. Schematic diagrams and illustration of (a) an energy landscape during a nucleation process, (b) conversion of a critical nucleus to a stable particle through atom attachment, and (c) nucleation rate as a function of temperature where T_0 is the transformation temperature.

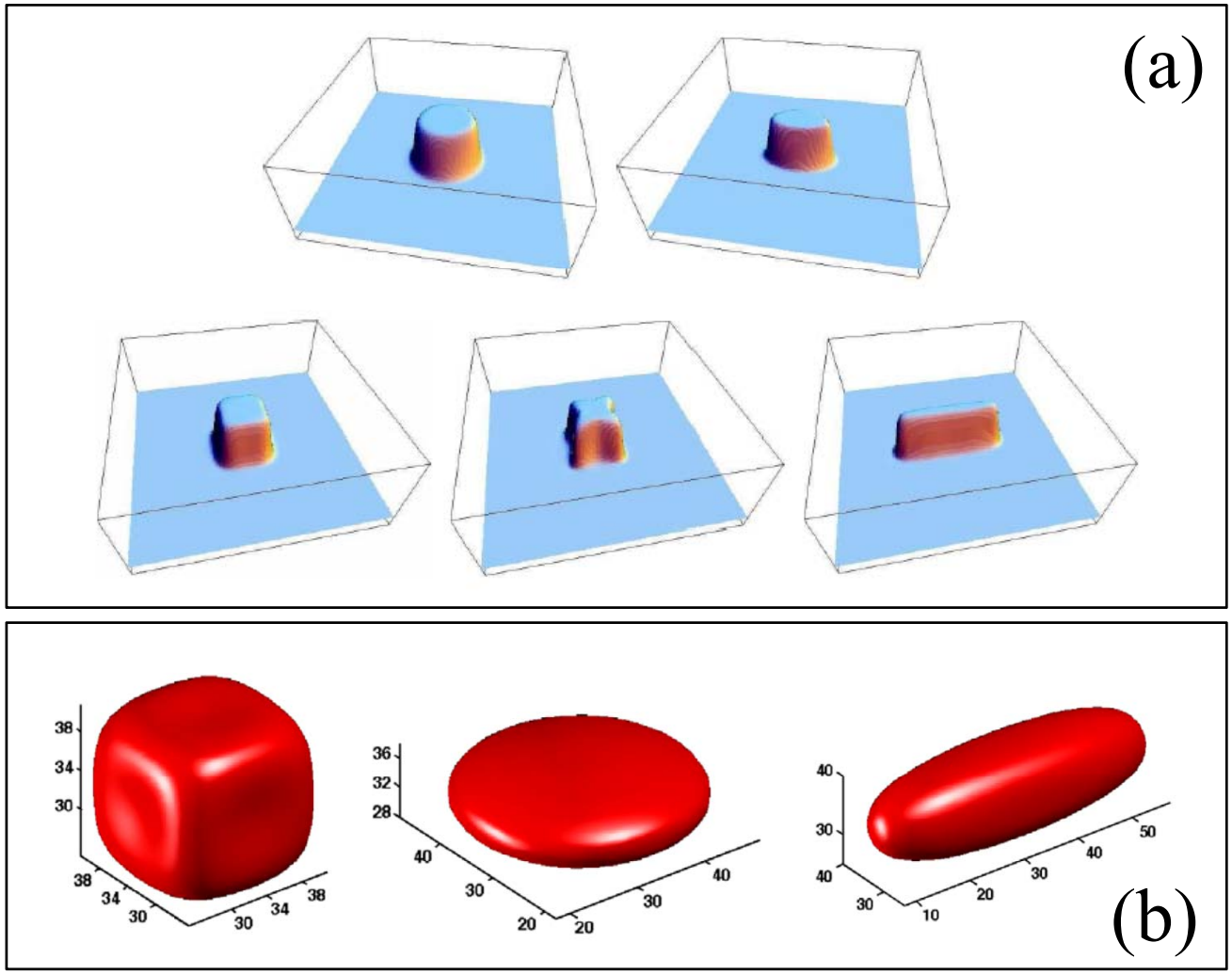

Figure 2. Critical nuclei profiles in (a) 2D systems [Zhang *et al*., *PRL*, **98**, 265703 (2007)] (Reprinted figure with permission from [40]. Copyright 2007 by the American Physical Society.) and (b) 3D systems [Zhang *et al*., *Acta Mater*., **56**, 3568 (2008)] predicted by the minimax algorithm (Reprinted with permission from [41]. Copyright 2008 by the Elsevier.).

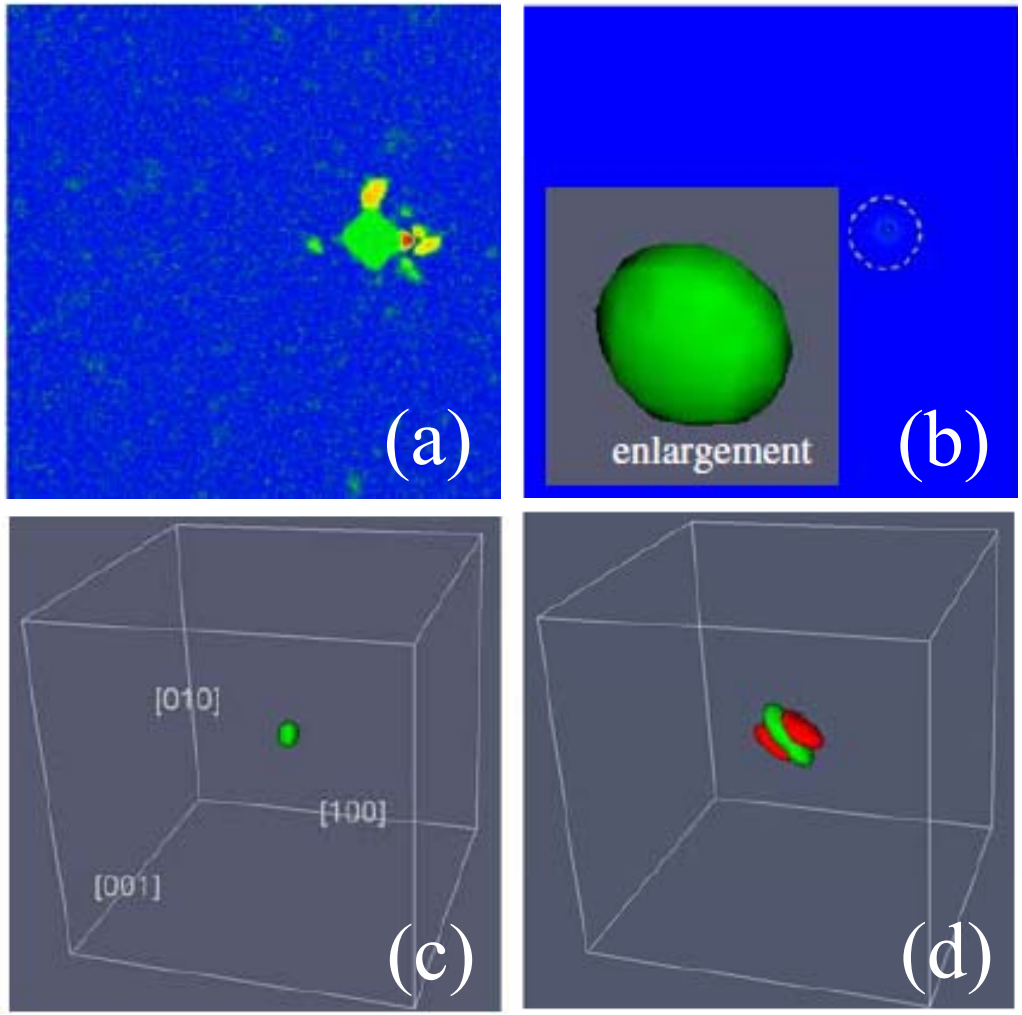

Figure 3. (a) A partially transformed state at an earlier stage of a cubic to tetragonal transformation in a 2D system produced by the Langevin dynamics, (b) a critical nucleus configuration in a 2D system, (c) a 3D critical nucleus with the low elastic energy contribution, and (d) a 3D critical nucleus with the high elastic energy contribution predicted by the free-end nudged elastic band method [Shen *et al.*, *MMTA*, **39A**, 976 (2008)]. Reprinted figure with permission from [43]. Copyright 2008 by the Springer.

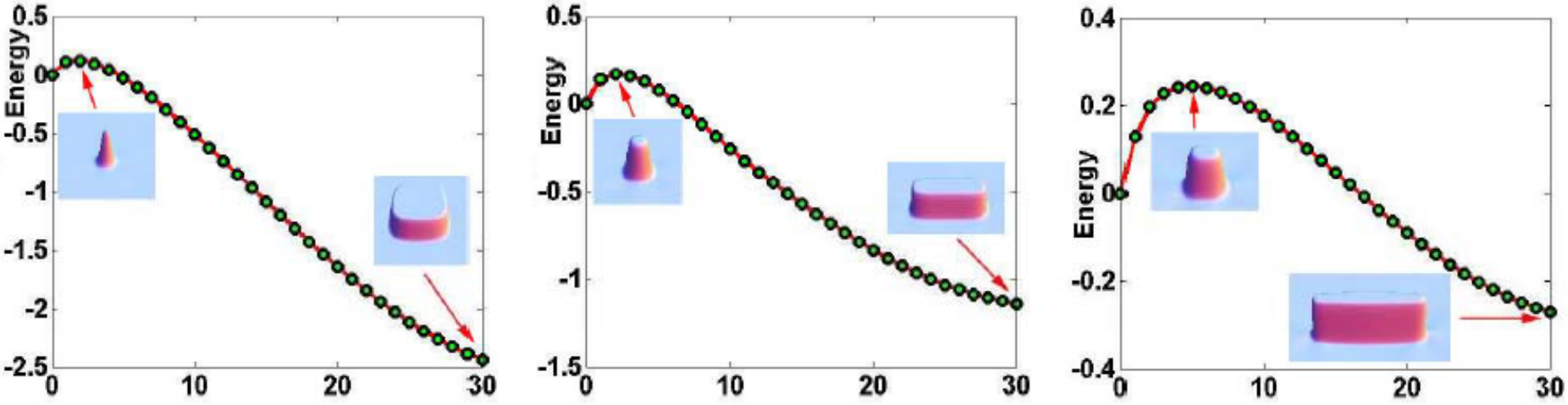

Figure 4. Minimum energy paths with a conservation constraint showing critical nuclei and equilibrium states for different elastic energy contributions predicted by the constrained string method [Zhang *et al*., *CICP*, **7**, 674 (2010)]. Reprinted figure with permission from [33]. Copyright 2010 by the Global Science Press.

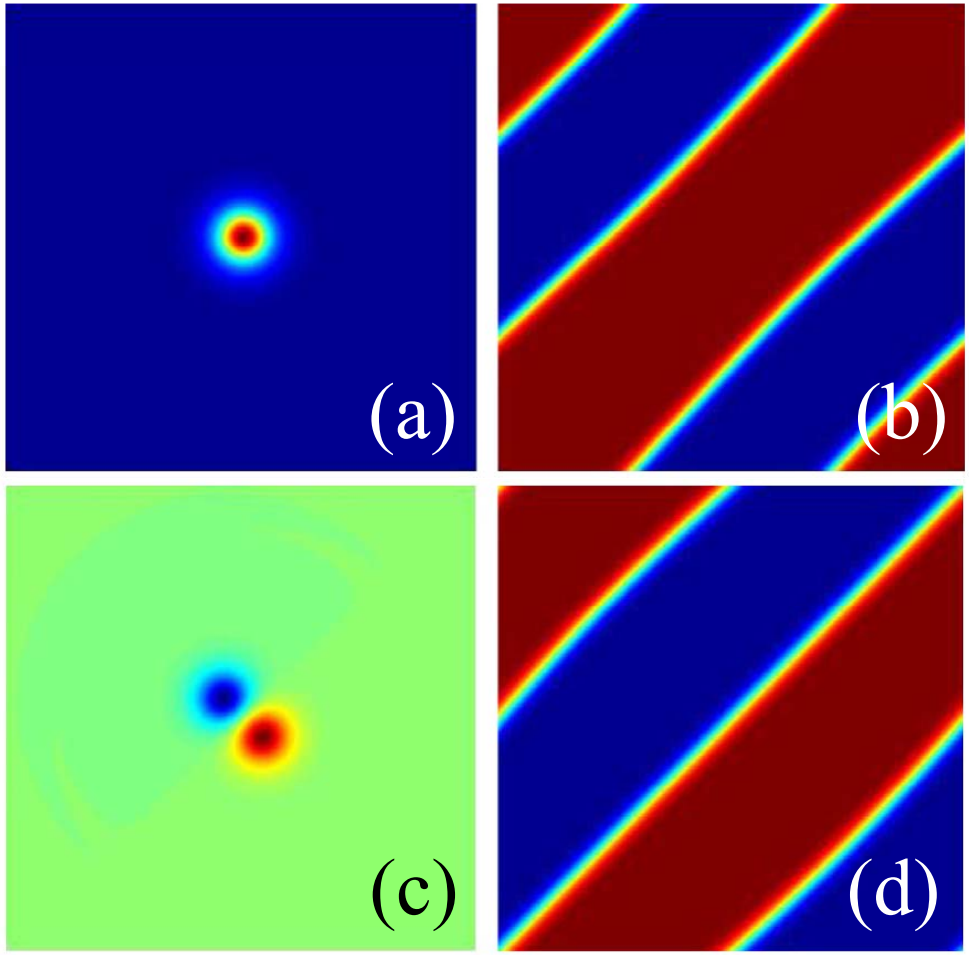

Figure 5. Application of the constrained string method to a cubic to tetragonal transformation with non-conserved phase-field variables: (a) critical nucleus and (b) equilibrium state profiles with the low elastic contribution, (c) critical nucleus and (d) equilibrium state profiles with the high elastic contribution [Zhang *et al*., *J. Comp. Phys.*, **229**, 6574 (2010)]. Reprinted figure with permission from [44]. Copyright 2010 by the Elsevier.

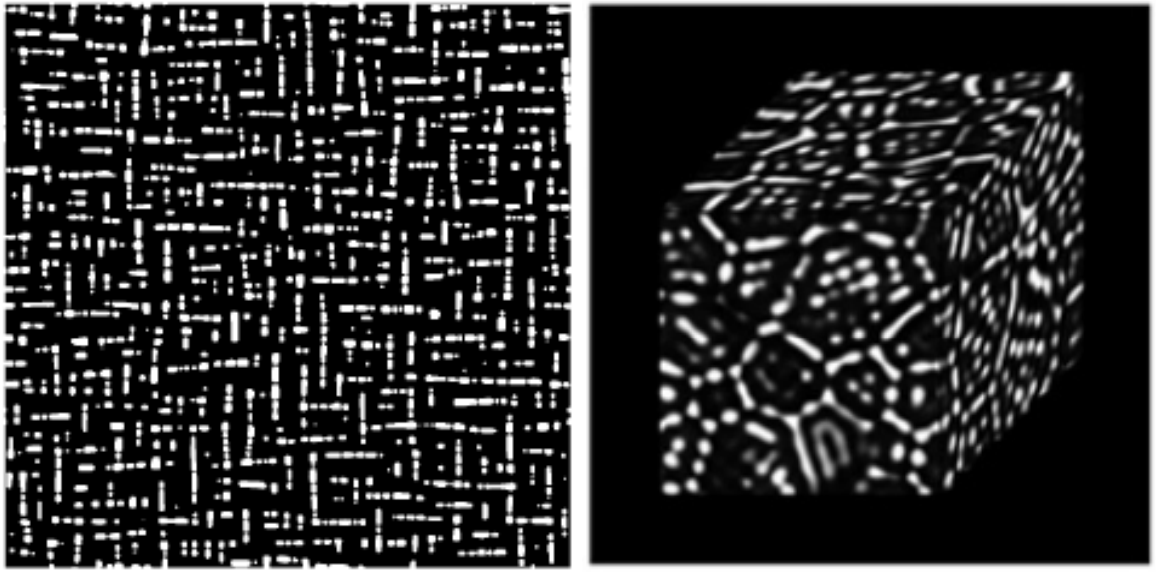

(a) (b)

Figure 6. Examples of nucleation driven by the Langevin noise in phase-field simulations: (a) nucleation during a *fcc* to $L1_2$ ordering process [Vaithyanathan *et al.*, *Acta Mater.*, **50**, 4061 (2002)] (Reprinted figure with permission from [47]. Copyright 2002 by the Elsevier.) and (b) precipitate nucleation during a generic diffusional process in a polycrystalline binary solid solution [Heo *et al.*, *Phil. Mag.*, **93**, 1468 (2013)] (Reprinted figure with permission from [48]. Copyright 2013 by the Taylor & Francis).

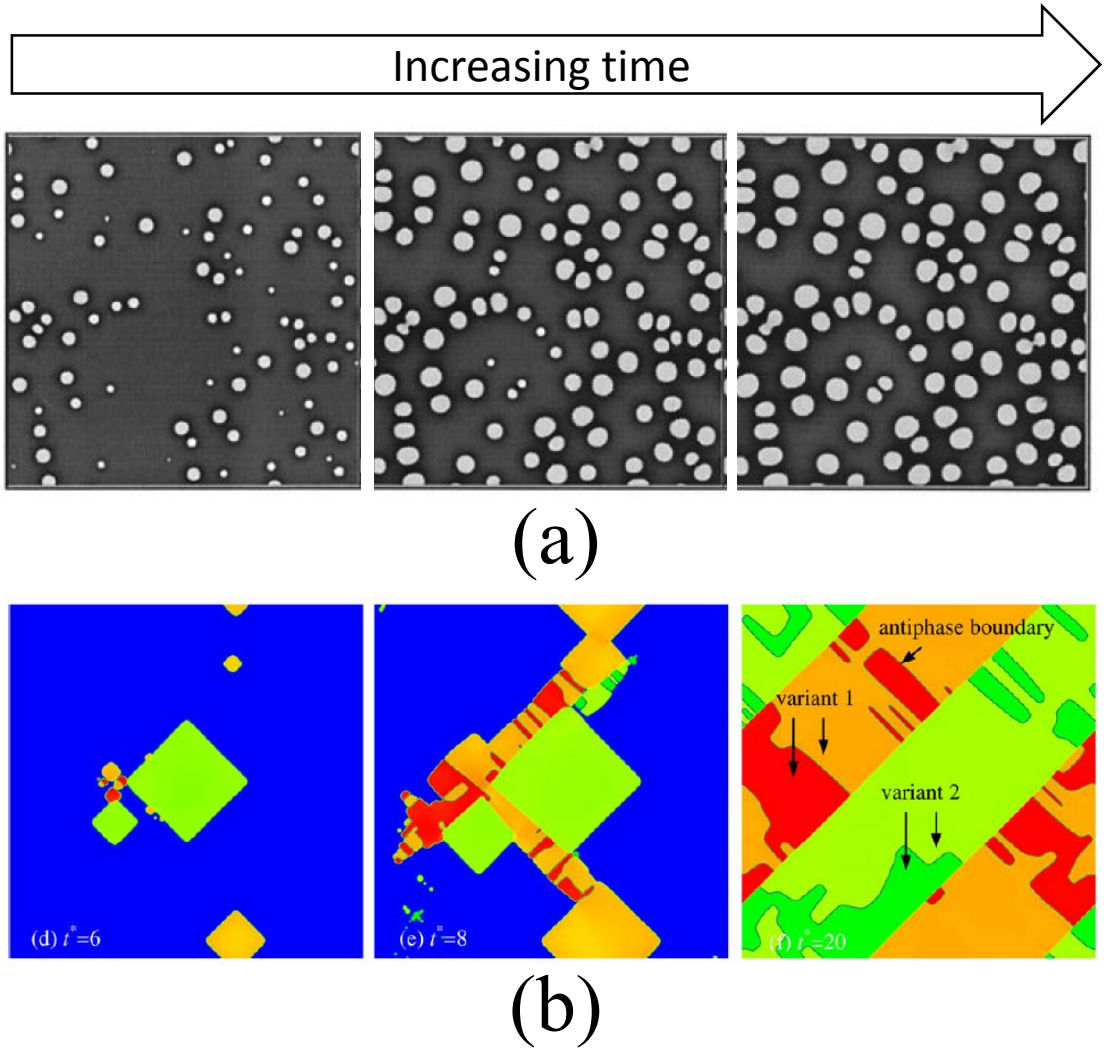

Figure 7. Examples of phase-field simulations of nucleation and growth with the explicit nucleation method and classical nuclei: (a) a generic nucleation and growth process [Simmons *et al*., *Scripta Mater*., **43**, 935 (2000)] (Reprinted figure with permission from [22]. Copyright 2000 by the Elsevier.) and (b) a cubic to tetragonal transformation [Shen *et al*., *Acta Mater*., **55**, 1457 (2007)] (Reprinted figure with permission from [51]. Copyright 2007 by the Elsevier.).

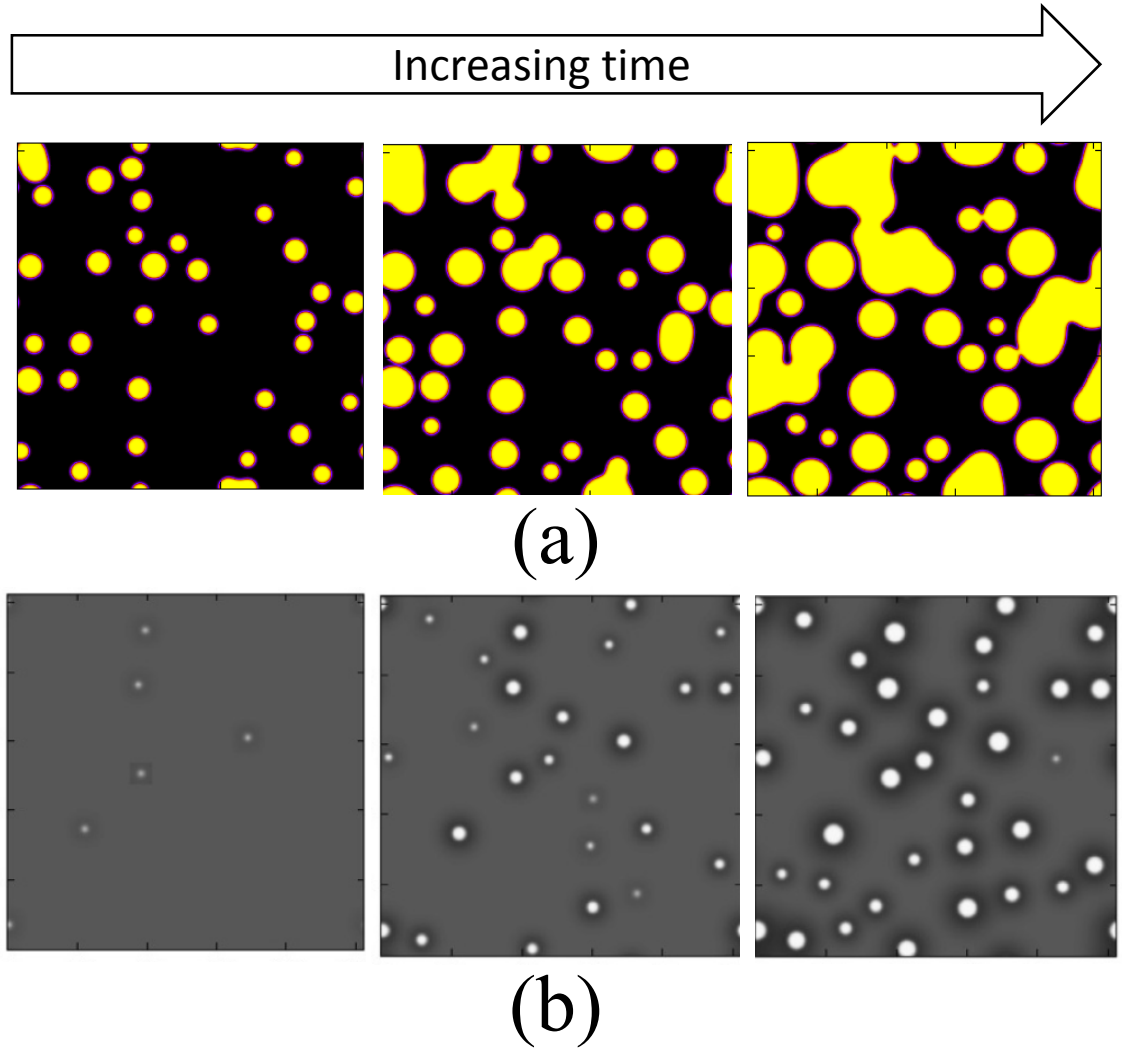

Figure 8. Examples of phase-field simulations of nucleation and growth with the explicit nucleation method and non-classical nuclei: (a) a generic structural transformation [Heo *et al*., *Scripta Mater*., **63**, 8 (2010)] (Reprinted figure with permission from [49]. Copyright 2010 by the Elsevier.) and (b) a generic phase transformation involving composition changes [Zhang, *Ph.D. Thesis*, The Pennsylvania State University (2009)] (Reprinted figure with permission from [52].).

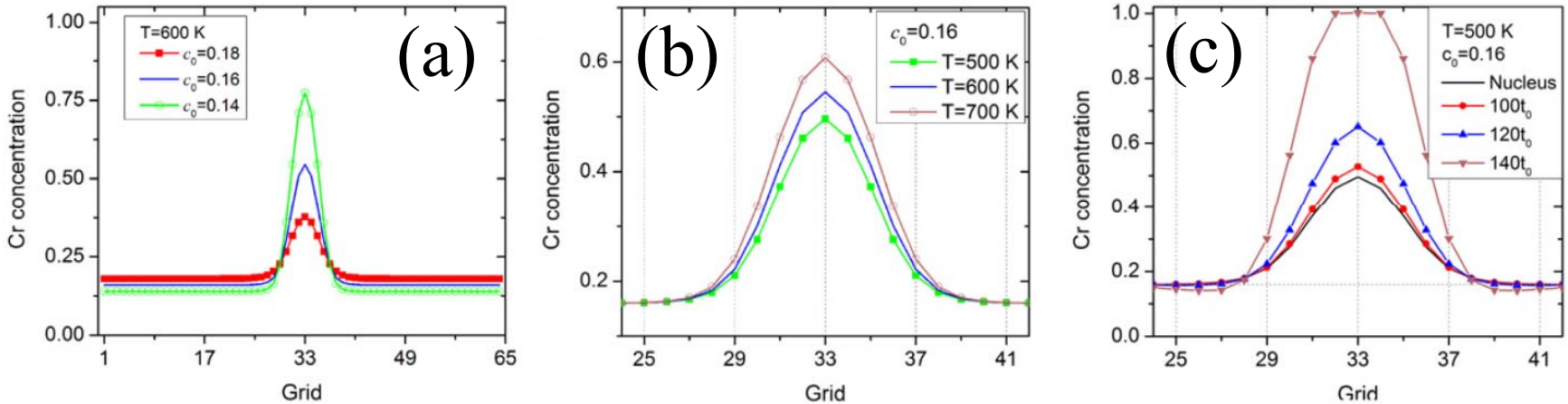

Figure 9. Critical nucleus profiles computed by the constrained shrinking dimer dynamic method for (a) different overall compositions of Cr and (b) different temperatures, and (c) the growth of the nucleus at 500 K when Cr overall composition is 0.16 [Li *et al*., *MSMSE*, **22**, 025002 (2014)]. Reprinted figure with permission from [53]. Copyright 2014 by the IOP Publishing.